

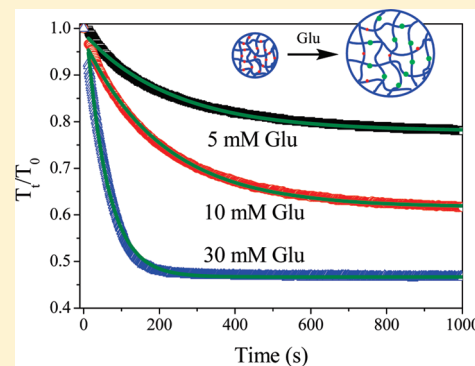
Kinetics of Glucose-Induced Swelling of P(NIPAM-AAPBA) Microgels

Shuying Xing, Ying Guan, and Yongjun Zhang*

State Key Laboratory of Medicinal Chemical Biology and Key Laboratory of Functional Polymer Materials, Institute of Polymer Chemistry, College of Chemistry, Nankai University, Tianjin 300071, China

Supporting Information

ABSTRACT: Rapid swelling is a major advantage of microgels over bulky gels, and chemical-induced swelling has been expected to occur on the same time scale as physically induced swelling. As an example, the kinetics of the glucose-induced swelling of poly(*N*-isopropylacrylamide-co-3-acrylamidophenylboronic acid) (P(NIPAM-AAPBA)) microgel was studied by turbidity. This process occurs on a time scale of 10^2 s, while the temperature-induced (de)swelling of PNIPAM microgels was reported to occur in time regime from 100 ns to tens of milliseconds. The slow glucose-induced swelling was attributed to the slow reaction between glucose and phenylboronic acid (PBA) groups, which was identified as the rate-determining step for microgel swelling. The rate constant of this reaction was further determined under various conditions and compared with that obtained in solution, using 3-aminophenylboronic acid as low molecular weight analogue. The reaction is accelerated when the microgels are in a swollen state, while it is retarded when the microgels are shrunken, revealing different effects of the polymer network on the reaction kinetics. Although the swelling rate of P(NIPAM-AAPBA) microgel is limited by the slow reaction between glucose and PBA groups, it is still much faster than the macroscopic hydrogel beads with same components (\sim several hours).



INTRODUCTION

Hydrogels are three-dimensional polymeric networks that swell in aqueous solutions without dissolving in them. Their swelling degree may change in response to small changes in their environment, such as temperature, pH, or ionic strength. These stimuli-responsive materials earned the reputation of intelligent or smart materials and have found applications in many fields especially in biomedical area.^{1,2} One major disadvantage of macroscopic hydrogels is their slow response rate. As Tanaka and Fillmore³ pointed out, the rate of gel swelling is dominated by the motion of polymer network. For spherical gel particles, the characteristic swelling time τ_{sw} is given by the equilibrium gel radius R_{eq} and the diffusion coefficient of the gel D_g :^{3,4}

$$\tau_{sw} = R_{eq}^2 / (\pi^2 D_g) \quad (1)$$

According to this relationship, one may effectively increase the swelling rate of a gel by reducing its size. For example, τ_{sw} will be reduced from $\sim 10^4$ s to $\sim 10^{-4}$ s when the gel radius is reduced from 1 mm to 100 nm, assuming D_g is on the order of 10^{-7} cm² s⁻¹.⁵ This result reveals that microgels can swell much faster than their macroscopic analogues, which is highly desirable for their application as smart drug carriers and biosensors. Some experimental studies also support this point. For example, Lyon et al.⁶ studied the dynamics of the temperature-induced deswelling and swelling of thermosensitive poly(*N*-isopropylacrylamide) (PNIPAM) microgels (diameter \sim 200 nm) using time-resolved transmittance measurements in combination with a nanosecond

laser-induced temperature-jump (T-jump) technique. They found the particle deswelling occurs on the microsecond time scale. Also using T-jump technique, Asher et al. found the temperature-induced shrinkage of PNIPAM microgels (diameter \sim 350 nm) embedded in hydrogel matrix occurs in the \sim 100 ns time regime.⁷ Recently Armes et al.⁸ reported that the characteristic times for pH-induced swelling of lightly cross-linked poly(2-vinylpyridine) latexes (diameter \sim 380–1010 nm) are of the order of tens of milliseconds.

Besides microgels responding to physical stimuli, microgels responding to chemical stimuli, for example, glucose,^{9,10} Pb²⁺¹¹ and K⁺,¹² are also designed and synthesized. These microgels swell to a different degree in response to a change in the concentration of the particular molecule in the milieu, therefore hold great promise for applications such as controlled drug delivery,¹³ sensing^{14,15} and chemically controlled gating.¹⁶ Their rapid responding rate is one of the most important merits for their use in these applications, however, to the best of our knowledge, no study on the kinetics of chemical-induced swelling of microgels has been reported yet. Researchers usually expect that chemical-induced microgel swelling occurs on the same time scale as the physically induced swelling.¹⁷

In this contribution we studied the kinetics of glucose-induced swelling of poly(*N*-isopropylacrylamide-co-3-acrylamidophenylboronic acid) (P(NIPAM-AAPBA)) microgel.⁹ We found it occurs

Received: March 15, 2011

Revised: April 27, 2011

Published: May 09, 2011

on a time scale of 10^2 s, which is several orders of magnitude slower than the temperature-induced (de)swelling of similar systems reported in the literature. We identified that the slow chemical reaction between glucose and PBA groups is the rate-determining step. The rate constants of this reaction under various conditions were further determined. Different effects of the polymer network on the reaction kinetics were revealed.

EXPERIMENTAL SECTION

Materials. *N*-Isopropylacrylamide (NIPAM) and β -D-(+)-glucose were purchased from Tokyo Chemical Industry Co., Ltd. *N,N'*-methylenebis(acrylamide) (BIS) and 3-aminophenylboronic acid (APBA) were purchased from Alfa Aesar. Acrylic acid (AA) and α -D-glucose were purchased from ACROS. Sodium dodecyl sulfate (SDS) was purchased from Sigma-Aldrich. *N*-(3-Dimethylaminopropyl)-*N'*-ethylcarbodiimide hydrochloride (EDC), potassium persulfate (KPS), D-(+)-Glucose and catechol were purchased from local providers. 3-Acrylamidophenylboronic acid (AAPBA) was synthesized as previously reported.¹⁸ NIPAM was purified by recrystallization from hexane/acetone mixture and dried in a vacuum. AA was distilled under reduced pressure. Other reagents were used as received.

Microgel Synthesis. Poly(*N*-isopropylacrylamide-co-acrylic acid) (P(NIPAM-AA)) microgel was synthesized as follows. 1.426 g of NIPAM, 0.103 g of AA, 0.043 g of BIS and 0.058 g of SDS were dissolved in 95 mL of water. The reaction mixture was transferred to a three-necked round-bottom flask equipped with a condenser and a nitrogen line. The solution was purged with nitrogen for 30 min and then heated to 70 °C. After 1 h, 5 mL of 0.06 M KPS solution was added to initiate the reaction. The reaction was allowed to proceed for 4 h. The resultant microgels were purified by dialysis (cutoff 8000–15000) against water with at least twice daily water changes for 2 weeks.

Poly(*N*-isopropylacrylamide-co-3-acrylamidophenylboronic acid) P-(NIPAM-AAPBA) microgel was prepared by modifying the P(NIPAM-AA) microgel with APBA as follows. 0.233 g of APBA was dissolved in 45 mL of water and added to 5 mL of purified P(NIPAM-AA) microgel. The mixture was cooled to ~ 4 °C with ice bath, to which 0.239 g of EDC was added. The reaction mixture was kept at about 4 °C for 4 h. The resultant products were purified by dialysis against water.

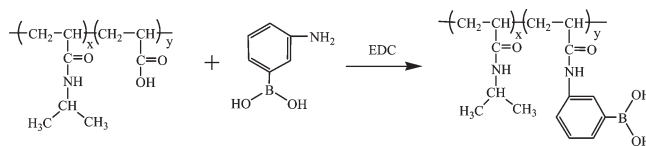
Titration. Lyophilized P(NIPAM-AA) microgel (0.05 g) was dissolved in 50 mL of water. The solution was bubbled with nitrogen and the pH was adjusted to 3.0 by adding HCl. It was titrated with standardized 0.1 N NaOH using a pH meter at 16 °C to determine the amount of AA. The amount of AAPBA in P(NIPAM-AAPBA) microgel was determined similarly.¹⁹

Dynamic Light Scattering. The hydrodynamic radii (R_h) of the microgel particles were measured by dynamic light scattering with a Brookhaven 90Plus laser particle size analyzer. All the measurements were carried out at a scattering angle of 90°. The sample temperature was controlled with a build-in Peltier temperature controller.

Turbidity. The turbidity of the diluted microgel dispersions, which is represented as the absorbance at 600 nm, was measured on a TU-1810PC UV–vis spectrophotometer (Purkinje General, China) using water as reference. Temperature was controlled with a refrigerated circulator. For kinetic studies, predetermined amount of glucose solution was quickly injected and mixed with 3 mL of microgel dispersion with an AAPBA concentration of 0.14 mM. The change in the turbidity of the dispersion was then recorded with time.

Rate Constant for Reaction of Glucose with APBA. The UV–vis spectra of APBA change slightly upon the addition of glucose because of the formation of APBA-glucose complex. Therefore the kinetics of the reaction between APBA and glucose can be measured by following the change in UV–vis spectra. In this study the absorbance at 300 nm, where the change is relatively large, was chosen to follow the

Scheme 1. Synthesis of P(NIPAM-AAPBA) Microgels by Modification of P(NIPAM-AA) Microgels with 3-Aminophenylboronic Acid



kinetics. The rate constant of the reaction was determined by measuring the change in absorbance of the sample at 300 nm with time.

Other Characterizations. Fourier transform infrared (FTIR) spectra were measured on a Bio-Rad FTS-6000 spectrometer. ¹H NMR spectra were recorded on a Varian UNITY-plus 400 NMR spectrometer using DMSO-*d*₆ and D₂O as solvent.

RESULTS AND DISCUSSION

Synthesis and Characterization of P(NIPAM-AAPBA) Microgels. Glucose-sensitive hydrogels can swell to a different degree in response to change in glucose concentration in the solution. These materials are synthesized typically based on the enzymatic oxidation of glucose by glucose oxidase,²⁰ binding of glucose with concanavalin A,²¹ or reversible covalent bond formation between glucose and boronic acids.²² They may find important applications in self-regulated insulin delivery and glucose sensing.²³ Recently we^{9,24,25} and others^{10,26} synthesized glucose-sensitive poly(*N*-isopropylacrylamide-co-3-acrylamidophenylboronic acid) (P(NIPAM-AAPBA)) microgel, using phenylboronic acid (PBA) as glucose-sensing moiety. Similar to their macroscopic analogues, these materials may have potential for self-regulated insulin release^{13,27,28} and glucose sensing.^{14,29}

P(NIPAM-AAPBA) microgels were synthesized by the modification of P(NIPAM-AA) microgels with 3-aminophenylboronic acid under EDC catalysis as reported previously (Scheme 1).⁹ The successful introduction of PBA groups is confirmed by the new peak at 8.08 ppm ($-B(OH)_2$ proton) and the peaks from 7.05 to 7.94 ppm (phenyl protons) in the NMR spectra of the modified microgel. (Supporting Information Figures 1S and 2S). The disappearance of the carboxylic acid proton peak (12.01 ppm) in NMR spectra and the absorption peak of carboxylic acid group (1711 cm^{-1}) in FTIR spectra (Supporting Information Figure 3S) indicate an almost complete conversion of the carboxylic acid groups.²⁵ The content of AA unit in the parent P(NIPAM-AA) microgel was determined to be $\sim 10.4 \pm 0.5$ mol % by pH titration (Supporting Information Figure 4S),¹⁹ which is equal to the AA content in the pregel solution.³⁰ Similarly the AAPBA content in the modified microgel was determined to be $\sim 11.0 \pm 0.5$ mol % (Supporting Information Figure 5S), which can be regarded as the same as AA content within the experimental error. These results confirm again an almost complete conversion of the carboxylic acid groups.

It is well-known that PNIPAM microgels are thermosensitive. They are highly swollen at low temperature, but undergo sharp volume phase transition at the lower critical solution temperature (LCST) of the PNIPAM polymer.³¹ Both P(NIPAM-AA) and P(NIPAM-AAPBA) microgels are thermosensitive too. As shown in Figure 1, when fully swollen, both microgels present a hydrodynamic radius (R_h) of ~ 140 nm. It reduces to ~ 60 nm when fully collapsed. The volume phase transition temperature (VPTT), defined as the onset of the phase transition, was determined

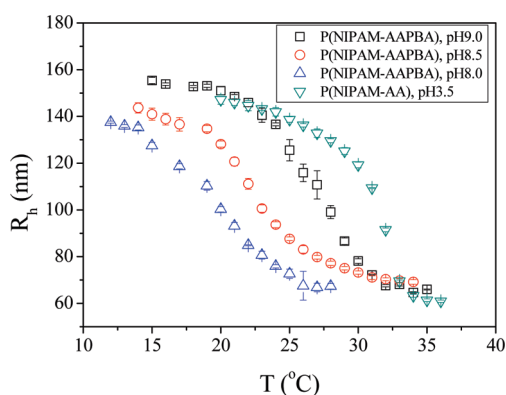


Figure 1. Hydrodynamic radii (R_h) of the parent P(NIPAM-AA) microgels and the corresponding P(NIPAM-AAPBA) microgels measured at various temperature. The P(NIPAM-AA) microgels are dispersed in pH3.5 water (∇), while the P(NIPAM-AAPBA) microgels are dispersed in 0.020 M phosphate buffer with a pH of 9.0 (\square), 8.5 (\circ), and 8.0 (Δ).

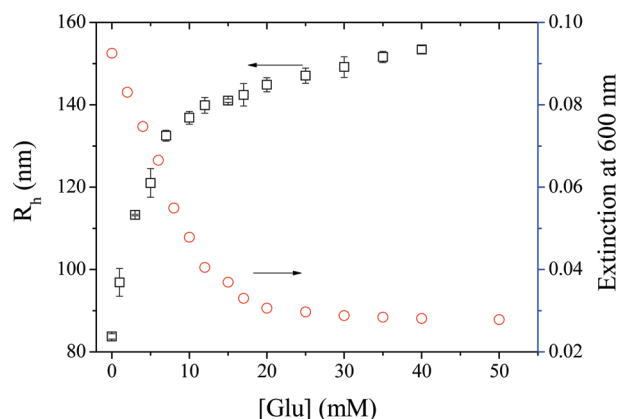
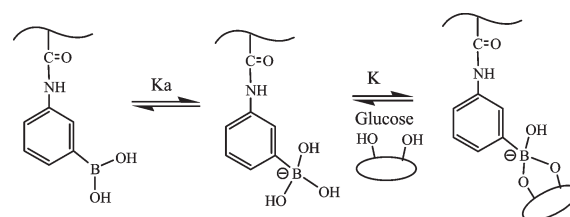


Figure 2. Hydrodynamic radii (R_h) (\square) and turbidity (\circ) of the P(NIPAM-AAPBA) microgels in 0.020 M pH 8.5 phosphate buffer containing various concentrations of glucose. $T = 25^\circ\text{C}$.

to be $\sim 30^\circ\text{C}$ for the parent P(NIPAM-AA) microgel (at pH 3.5), and $\sim 18^\circ\text{C}$, $\sim 20^\circ\text{C}$ and $\sim 24^\circ\text{C}$ for the corresponding P(NIPAM-AAPBA) microgels at pH 8.0, 8.5, and 9.0, respectively. The decrease in VPTT upon modification is attributed to the replacement of the hydrophilic monomer AA with the hydrophobic monomer AAPBA.⁹ Increasing VPTT of P(NIPAM-AAPBA) microgel with increasing pH is attributed to a higher degree of dissociation of PBA groups at a higher pH. As we showed previously, the P(NIPAM-AAPBA) microgel swells to a larger degree in the presence of glucose. (Figure 2) The glucose-sensitivity originates from the binding of glucose with PBA groups which converts more PBA groups from the neutral, hydrophobic form to negatively charged, hydrophilic form (Scheme 2).²² Simultaneously, the turbidity of the microgel dispersion decreases with increasing glucose concentration (Figure 2). As the microgel particles swell to a larger degree in the presence of glucose, their refractive index decreases, which dominates over the size factor in determining the scattering efficiency, thus resulting in a lower turbidity.^{14,32}

Kinetics of Glucose-Induced Microgel Swelling. The swelling kinetics of a macroscopic gel can be facilely followed by

Scheme 2. Complexation Equilibrium between Phenylboronic Acid Derivative and Glucose



measuring its size change. Specially, the swelling kinetics of P(NIPAM-AAPBA) hydrogel beads with a size of 0.2–0.8 mm has been studied by monitoring its size change under microscope.³³ These hydrogel beads take several hours to fully swell in 5 g/L glucose solution. Asher et al.³⁴ studied the glucose-induced deswelling of a PBA-containing hydrogel membrane with a thickness of $\sim 125\ \mu\text{m}$.³⁵ 90% of the deswelling occurs within ~ 15 and ~ 90 min in response to the introduction of 10 and 1 mM β -D-glucose, respectively. In contrast, the study of the swelling kinetics of microgels is much difficult. Advanced techniques are required to monitor their quick swelling.⁵ Even this process can be followed by certain technique, it is still difficult to directly measure the size change with time. As a result experimental researches in this area are relatively rare.^{5,6,8,36} Without exception, instead of size change, the changes in turbidity^{6,8,36} or scattered light intensity⁵ were monitored with time.

Here, we also monitor the turbidity change of the microgel dispersions to study the kinetics of the glucose-induced microgel swelling. As shown in Figure 3A, upon the addition of glucose, the turbidity of the microgel dispersions drops immediately and levels off gradually. The kinetic curves can be well-fitted with the following single-exponential function:

$$A = A_0 + B \exp(-t/\tau_{\text{sw}}) \quad (2)$$

The characteristic swelling time τ_{sw} can thus determined to be 223.9 ± 9.5 , 169.0 ± 1.7 , 122.0 ± 2.3 , 100.1 ± 2.9 , and 59.2 ± 2.0 s, for the five glucose concentrations (5, 10, 15, 20, and 30 mM) studied here, respectively. Recently Liu et al.⁵ used the same method to determine τ_{sw} for the pH-induced deswelling of poly(2-vinylpyridine) microgels. The swelling or deswelling kinetics of some other hydrogels^{37,38} was also found to follow a single-exponential behavior.

The results reveal two features of the glucose-induced swelling. First, a higher concentration of glucose not only result in a higher degree of swelling, as indicated by the larger decrease in turbidity, but also a faster swelling rate, as indicated by the shorter characteristic swelling time. Second, the glucose-induced swelling of P(NIPAM-AAPBA) microgel is much slower than the swelling or deswelling of other microgels reported in the literature.^{6–8} It is 4 orders of magnitude slower than the acid-induced swelling of poly(2-vinylpyridine) (P2VP) latex particles,⁸ and 8–10 orders of magnitude slower than the temperature-induced deswelling of PNIPAM microgels.^{6,7} At first glance, these results are quite unexpected.

The swelling of the P(NIPAM-AAPBA) microgel upon the addition of a chemical can be regarded as a consequence of three different processes: (1) diffusion of the chemical into the microgel particles, (2) reaction between the chemical and the PBA functional groups, and (3) structural rearrangements of the gel due to

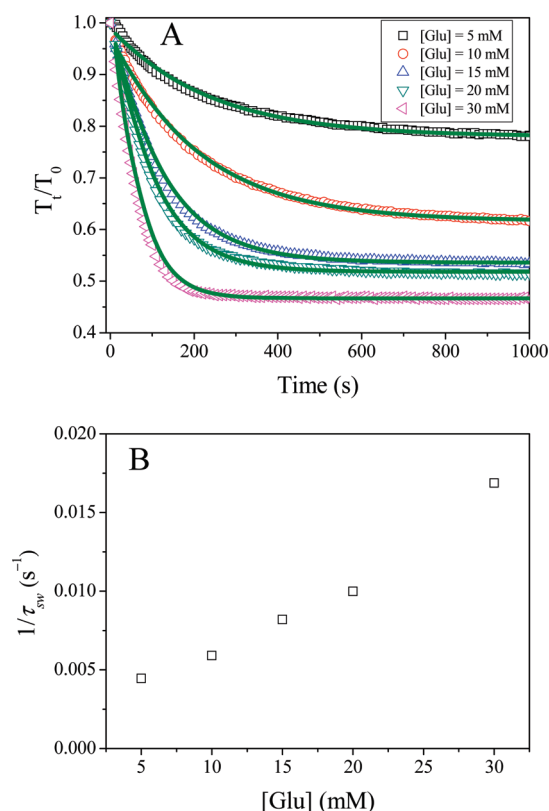


Figure 3. (A) Relative turbidity of P(NIPAM-AAPBA) microgel dispersion changes with time upon addition of glucose. The media were 0.020 M pH8.5 phosphate buffer. $T = 25$ °C. The solid lines show the best single exponential fits to the data. (B) Reciprocal of the characteristic swelling time, $1/\tau_{sw}$, as a function of glucose concentration.

the changed property of the polymer chains, which results in the (de)hydration and (de)swelling of the gel.

The first step, that is, the diffusion of a low molecular weight chemical, such as glucose, into the microgel particles, is supposed to be fast. Assuming that the diffusion constant of glucose in polyacrylamide hydrogel is similar to that in water (5.2×10^{-6} cm²/s at room temperature), Asher et al. estimated the characteristic time for glucose diffusing into a 100 μ m thickness hydrogel film is ~ 10 s.³⁴ For the diffusion of glucose into a spherical microgel particle with a radius of 100 nm, the characteristic time τ_{sp} is estimated to be $\sim 10^{-5}$ s ($\tau_{sp} = R^2/(\pi^2 D)$, where R is the radius and D the diffusion constant³⁹). Even if the diffusion constant of glucose inside PNIPAM microgel is 100-fold smaller than that in water, the calculated characteristic time for glucose diffusing ($\sim 10^{-3}$ s) is still much smaller than the characteristic time for the microgel swelling. Therefore the fast diffusion of glucose should not be the rate-determining step for microgel swelling.

The third step, that is, the structural rearrangements of the microgel, is very fast too. As mentioned above, the characteristic swelling time τ_{sw} is estimated to be $\sim 10^{-4}$ s for spherical microgel particles with a radius of 100 nm,⁵ according to the theoretical model of Tanaka and Fillmore.^{3,4} Therefore, the fast structural rearrangements of the gel should not be the rate-determining step either. The only possible rate-determining step should be the chemical reaction between glucose and PBA groups.

This hypothesis is supported by the linear relationship between the microgel swelling rate and glucose concentration, as shown in Figure 3B, where the microgel swelling rate is represented

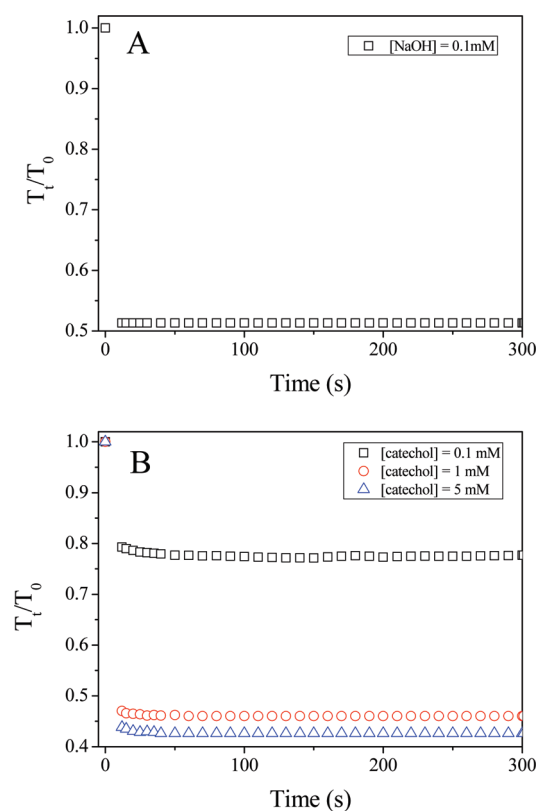


Figure 4. Relative turbidity of the P(NIPAM-AAPBA) microgel dispersion changes with time upon addition of NaOH (A), and catechol (B). The media were water (A) and 0.050 M pH8.5 phosphate buffer (B), respectively. $T = 25$ °C.

by the reciprocal of the characteristic swelling time, $1/\tau_{sw}$. An increase in glucose concentration results in an increase in the reaction rate between glucose and PBA, which in turn results in an increase in the swelling rate of the microgel.

For comparison, the swelling kinetics of the P(NIPAM-AAPBA) microgel upon addition of NaOH and catechol were also studied. PBA is a weak acid with a pKa of ~ 8.2 .⁴⁰ The addition of NaOH results in the dissociation of the PBA groups, which in turn results in the swelling of the microgel. Catechol, which bears diol group, can bind with PBA groups in the same way as glucose (but with a higher affinity⁴¹), and thus result in the swelling of the microgel. As shown in Figure 4A, the NaOH-induced swelling is too fast to be followed using the same method, while the catechol-induced swelling can only be partially followed (Figure 4B). These results further confirm the slow glucose-induced swelling of P(NIPAM-AAPBA) microgel should be attributed to a slow reaction rate between glucose and PBA.

Determination of Rate Constant of the Reaction between Glucose and PBA in the Microgel. Since the reaction between glucose and PBA groups is recognized as the rate-determining step, next we will try to determine the rate constant of the reaction. The reaction between PBA and glucose can be represented as



The reaction rate can be written as:

$$-\frac{d[\text{PBA}]}{dt} = k[\text{PBA}][\text{Glu}] - k_{-1}[\text{PBA-Glu}] \quad (4)$$

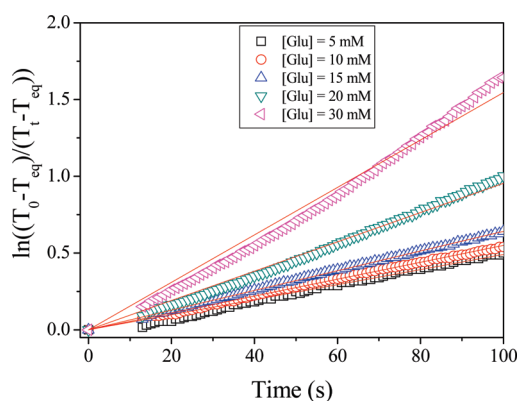


Figure 5. Replot of the swelling kinetics data in Figure 3A according to eq 9.

where k and k_{-1} are rate constants for the forward and reverse reactions, respectively. When $[\text{Glu}]_0 \gg [\text{PBA}]_0$, the change in $[\text{Glu}]$ will be negligible. So eq 4 can be rewritten as

$$-\frac{d[\text{PBA}]}{dt} = k_a[\text{PBA}] - k_{-1}[\text{PBA-Glu}] \quad (5)$$

where $k_a = k[\text{Glu}]_0$. In this case, the reaction is similar to the mutarotation of glucose (interconversion of α - and β - anomers) in water. The reaction rate constants can be determined using the similar relations:⁴²

$$\ln\left(\frac{[\text{PBA}]_0 - [\text{PBA}]_{\text{eq}}}{[\text{PBA}]_t - [\text{PBA}]_{\text{eq}}}\right) = (k_a + k_{-1})t = k_{\text{app}}t \quad (6)$$

$$K = \frac{k}{k_{-1}} \quad (7)$$

where K is the equilibrium constant, and $k_{\text{app}} = k_a + k_{-1}$. So, we get the following relationship:

$$k_{\text{app}} = k[\text{Glu}]_0 + \frac{k}{K} \quad (8)$$

To determine k_{app} or k , one may measure the change of $[\text{PBA}]$ with time directly. However, it is difficult to do so. Here we hypothesize that the change of $[\text{PBA}]$ can be represented by the change of turbidity of the dispersion. Therefore eq 6 was rewritten as

$$\ln\left(\frac{T_0 - T_{\text{eq}}}{T_t - T_{\text{eq}}}\right) = (k_a + k_{-1})t = k_{\text{app}} \cdot t \quad (9)$$

where T_0 , T_t , and T_{eq} are the turbidity (represented as absorbance at 600 nm) of the microgel dispersion at the beginning, time t , and after equilibrium.

On the basis of the hypothesis, the kinetics data of the initial stage shown in Figure 3A were replotted according to eq 9. As shown in Figure 5, good linear relationship was obtained, suggesting the hypothesis is reasonable. (A slight upturn was observed in the cases of $[\text{Glu}] = 20$ mM and 30 mM, which can be explained by a slight increase in the rate constant as the microgel swelling, as the polymer effect on the reaction changes with the swelling degree of the microgel.) From the slope of the fitted line, k_{app} values at various $[\text{Glu}]$ are determined according to eq 9. Subsequently k_{app} is plotted against $[\text{Glu}]$ as shown

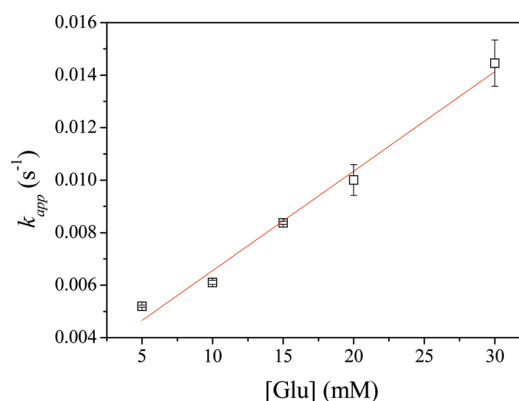


Figure 6. Determination of reaction constant k according to eq 8.

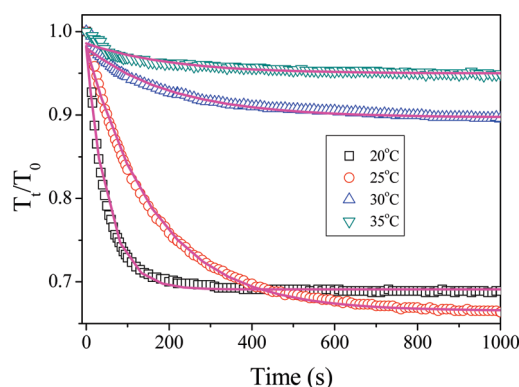


Figure 7. Relative turbidity of the P(NIPAM-AAPBA) microgel dispersion changes with time upon addition of 10 mM glucose. The media were 0.020 M pH8.5 phosphate buffer. The temperature is 20 (\square), 25 (\circ), 30 (Δ), and 35 $^{\circ}\text{C}$ (∇). The solid lines show the best single exponential fits to the data.

in Figure 6. The reaction rate constant k is determined from the slope of the fitted line, which is $0.379 \text{ M}^{-1} \cdot \text{s}^{-1}$ when measured in 0.020 M pH8.5 phosphate buffer at 25 $^{\circ}\text{C}$. Using this method, the rate constants of the reaction between PBA and glucose under various conditions were measured. Each measurement was repeated for at least three times. The average values and the standard errors were reported.

Effect of Temperature. The kinetics of the glucose-induced swelling of P(NIPAM-AAPBA) microgel was studied at various temperatures. The same 0.020 M pH8.5 phosphate buffer was used as media. Figure 7 shows the swelling kinetics of P(NIPAM-AAPBA) microgel upon addition of 10 mM glucose. At different temperature, the degree of swelling is different, so is the swelling rate. From single-exponential fitting, the characteristic swelling times at a final $[\text{Glu}]$ of 10 mM were obtained to be 51.4 ± 1.6 s (20 $^{\circ}\text{C}$), 169.0 ± 1.7 s (25 $^{\circ}\text{C}$), 209.4 ± 0.1 s (30 $^{\circ}\text{C}$) and 202.8 ± 0.4 s (35 $^{\circ}\text{C}$), respectively, indicating the glucose-induced swelling slows down with increasing temperature. (Figure 8) The swelling of the microgel under physiological conditions may be even slower because of higher temperature and ionic strength.

The reaction rate constant between glucose and PBA in the microgels at various temperatures was determined as described above. As shown in Figure 8, with increasing temperature, the microgel swelling rate and the reaction rate follow the same trend. For comparison, reaction rate constant between glucose and

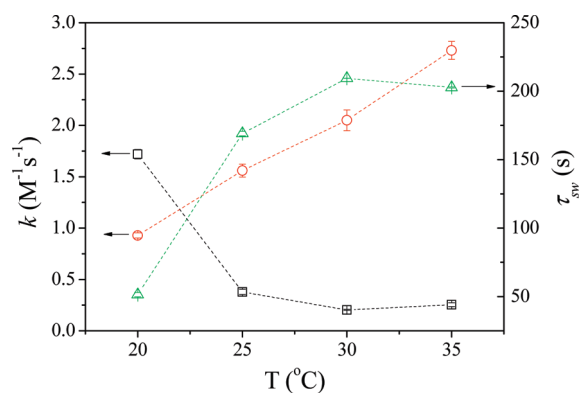


Figure 8. Rate constant for reaction of glucose with PBA groups in microgel (□) and APBA (○) and the characteristic swelling time of P(NIPAM-AAPBA) microgel at a final [Glu] of 10 mM at various temperatures (Δ). The media were 0.020 M pH 8.5 phosphate buffer. The dashed lines are included to guide the eye.

APBA, as a low molecular weight analogue, was also determined. As shown in Figure 8, the reaction rate between glucose and APBA increases with temperature. The apparent activation energy of the reaction was calculated to be ~ 52.8 KJ/mol according to Arrhenius equation (Supporting Information Figure 4S).

From Figure 8, one can see that immobilization of PBA groups on microgel network accelerates their reaction with glucose at 20 °C, while retards the reaction at higher temperature. It has long been recognized that the attachment of a functional group to macromolecules will influence its reaction with low molecular weight species.⁴³ Usually one can assume the immobilized functional group has the same reactivity as its low molecular weight analogues and attribute the difference to various factors induced by the polymer backbone, including steric hindrance, microenvironment, the interaction between the polymer backbone and the low molecular weight species⁴⁴ and the effect of neighboring groups.⁴⁵ These factors may either accelerate or retard the reaction, and the final result should be the combined effects of all these factors. The acceleration of the reaction at 20 °C may be attributed to the relative hydrophilicity of the polymer and the relatively large swelling degree of the network under this condition (see Figure 1). The large swelling degree of microgel allows for glucose to diffuse freely into the microgel to access PBA groups inside. Because of the hydrophilicity of the polymer, the microenvironment of PBA groups attached may be similar to those dissolved in water. As a result the retardation effect from the polymer may not be severe in this case. On the other hand, since the PBA groups are concentrated inside the microgel spheres, which results in an increased local PBA concentration, the reaction rate may increase accordingly. Another possible reason for the accelerated reaction may be the accumulation of glucose molecules on the hydrophilic PNIPAM chains through hydrogen-bonding.⁴⁶ Recently Ballauff et al.⁴⁷ also reported that the enzymatic activity of β -D-glucosidase immobilized in PNIPAM networks is increased compared to its activity in solution.

The retarded reaction at higher temperatures may be attributed to reduced accessibility of PBA groups because the microgel is partially or fully shrunk under these conditions (see Figure 1). The functional PBA groups may be buried because of the polymer conformation change. Previously Frere and Gramain⁴⁸ showed that the quaternization of poly(vinylpyridine) is retarded and even stopped when the polymer conformation changes from coil to

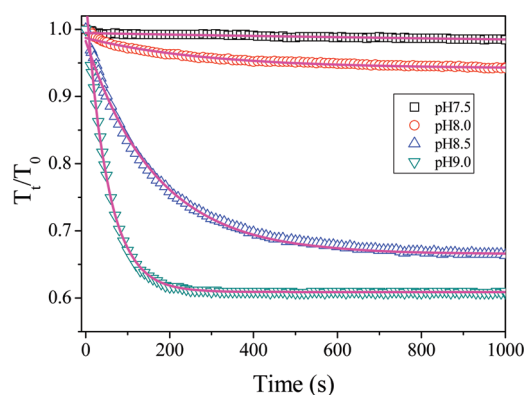


Figure 9. Relative turbidity of the P(NIPAM-AAPBA) microgel dispersion changes with time upon addition of 10 mM glucose. The media were 0.020 M phosphate buffer with a pH of 7.5 (□), 8.0 (○), 8.5 (Δ), and 9.0 (▽). $T = 25$ °C. The solid lines show the best single exponential fits to the data.

globule. In addition, as the polymer becomes more and more hydrophobic, the microenvironment of PBA group changes accordingly, which may also results in a reduced reactivity.^{44,49} The degree of retardation ($k_{\text{APBA}}/k_{\text{microgel}}$) increases from 4.1 (25 °C) to 10.0 (30 °C) and 10.7 (35 °C) is in accord with the fact that the microgels become more hydrophobic and shrink to a larger degree as temperature rising. The thermal phase transition of PNIPAM microgel has previously been used to tune the catalytic activity of nanoparticles^{50,51} or other catalytic active site⁵² immobilized inside the microgels.

Effect of pH. The kinetics of the glucose-induced swelling of P(NIPAM-AAPBA) microgel at 25 °C and various pHs were studied. Figure 9 shows the kinetics curves measured at different pHs while the glucose concentration keeps constant (10 mM). At pH 7.5, the extent of reaction is rather low, which is in agreement with previous reports.⁴¹ No reliable characteristic swelling time was obtained from single-exponential fitting. For other pHs, the characteristic swelling times were determined to be 280.0 ± 2.7 s (pH 8.0), 169.0 ± 1.7 s (pH 8.5), and 47.7 ± 1.5 s (pH 9.0). One can see that the microgel swells faster at higher pH.

Similarly, rate constant of the reaction between glucose and PBA in the microgels at different pHs were determined (Figure 10). We failed to determine a reliable rate constant at pH 7.5 because of the low extent of reaction. Again, the microgel swelling rate and the reaction rate were found to follow the same trend with changes in pH. For comparison, rate constants of the reaction between glucose and APBA under the same conditions were determined (Figure 10). It is well-known that the binding constant between PBA and glucose is pH dependent,^{35,41} however, the reaction kinetic is much less dependent on pH. The reaction rate between APBA and glucose only slightly increases with pH. With the attachment of PBA on PNIPAM microgels, a retardment was observed at pHs 8.0 and 8.5, while an acceleration was observed at pH 9.0, revealing different polymer effects at different pHs. The retardment at pHs 8.0 and 8.5 can be attributed to the hydrophobicity of the polymer and the shrinkage of the microgel under these conditions (see Figure 1), as explained above. In contrast, as more PBA groups are dissociated at pH 9.0, the polymer becomes more hydrophilic, and the microgel swells to a larger degree. Actually the swelling degree of the microgel in this case (pH 9.0, 25 °C) is similar to that in the case of pH 8.5 and 20 °C discussed above (the R_h is ~ 126 nm in

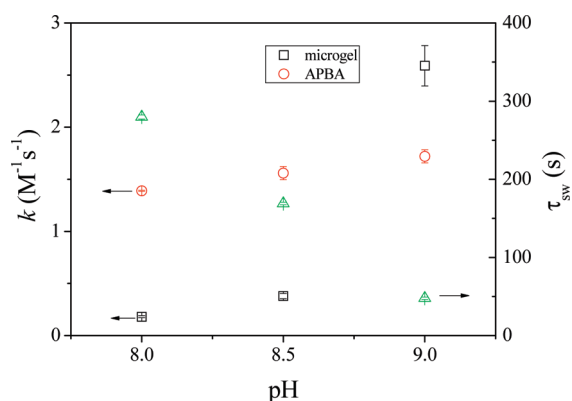


Figure 10. Rate constant for reaction of glucose with PBA groups in microgel (\square) and APBA (\circ) and the characteristic swelling time of P(NIPAM-AAPBA) microgel at a final $[\text{Glu}]$ of 10 mM (Δ) at various pHs. The media were 0.020 M phosphate buffer. $T = 25^\circ\text{C}$.

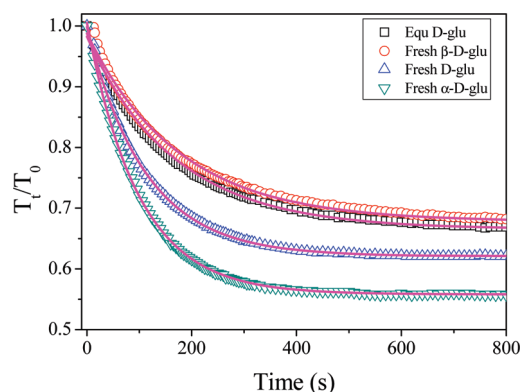


Figure 11. Relative turbidity of the P(NIPAM-AAPBA) microgel dispersion changes with time upon addition of equilibrated D-glucose (\square), fresh β -D-glucose (\circ), fresh D-glucose (Δ), or fresh α -D-glucose (∇). The final concentrations of glucose were all 0.010 M. The media were 0.020 M pH 8.5 phosphate buffer. $T = 25^\circ\text{C}$. The solid lines show the best single exponential fits to the data.

both cases as shown in Figure 1). Therefore the acceleration of the reaction can be explained similarly.

Effect of Glucose Mutarotation. In the above studies, the D-glucose solutions were all stood overnight before use to ensure that they had reached mutarotation equilibrium. As we know, D-glucose exists in aqueous solution in many different isomers. At equilibrium, the solution is actually a mixture of β -D-glucopyranose and α -D-glucopyranose with traces of the other forms including furanoses and open-chain form. The swelling kinetics P(NIPAM-AAPBA) microgel in the presence of various types of glucose was studied. As shown in Figure 11, the swelling rate induced by various types of isomers is different, which increases in the order of fresh β -D-glucose < equilibrated D-glucose < fresh D-glucose < fresh α -D-glucose. The characteristic swelling times upon the addition of 10 mM of these sugars are determined to be 178.0 ± 6.4 , 169.0 ± 1.7 , 110.9 ± 1.5 , and 95.7 ± 3.4 s, respectively. Previously Asher et al also found that their glucose-sensitive hydrogel response to various type of glucose in the same order.³⁴ Using the above method, the reaction rate constants between PBA groups and different types of glucose were determined, which are 0.241 ± 0.0177 (fresh- β -D-glucose),

0.379 ± 0.0254 (equilibrated D-glucose), 0.903 ± 0.0521 (fresh D-glucose) and $0.962 \pm 0.0760 \text{ M}^{-1}\cdot\text{s}^{-1}$ (fresh α -D-glucose), respectively. As Asher et al.³⁴ pointed out, α -D-glucose reacts with PBA faster than β -D-glucose because glucose binds with PBA in the α -furanose or α -pyranose form(s).^{53,54} Their affinity to the immobilized PBA follows the same order. As the rate constant of fresh D-glucose is close to that of fresh α -D-glucose, the D-glucose sample we used is actually primarily in the α -form. The equilibrated D-glucose is a mixture of the β -form and the α -form, therefore its rate constant is larger than β -D-glucose but less than α -D-glucose.

CONCLUSIONS

As an example, the kinetics of the glucose-induced swelling of P(NIPAM-AAPBA) microgel was studied by turbidity. This process occurs on a time scale of 10^2 s, which is several orders of magnitude slower than the temperature-induced volume transition of PNIPAM microgels. The unexpected slow swelling originates from the slow reaction between glucose and PBA groups, which was identified as the rate-determining step for the swelling process.

Based on these observations, a chemical-induced microgel swelling may not be as fast as we expected before, however, the swelling of a microgel is still much faster than the swelling of its bulky analogues. As already mentioned, it takes several hours for macroscopic hydrogel beads of P(NIPAM-AAPBA) to fully swell in the presence of glucose,³³ which is much slower than microgels with similar composition. The relatively quick swelling of P(NIPAM-AAPBA) microgels still makes them better choice for application in drug delivery and biosensor.

ASSOCIATED CONTENT

Supporting Information. NMR spectra of the microgels and monomer AAPBA, FTIR spectra and titration curves of the microgels, and temperature dependent rate constant for reaction of glucose with APBA. This material is available free of charge via the Internet at <http://pubs.acs.org>.

AUTHOR INFORMATION

Corresponding Author

*E-mail: yongjunzhang@nankai.edu.cn.

ACKNOWLEDGMENT

We thank financial support for this work from and the National Natural Science Foundation of China (Grants No. 20774049 and 20974050) and the Ministry of Science and Technology of China (Grant No.: 2007DFA50760).

REFERENCES

- (1) Roy, D.; Cambre, J. N.; Sumerlin, B. S. *Prog. Polym. Sci.* **2010**, 35, 278–301.
- (2) Mano, J. F. *Adv. Eng. Mater.* **2008**, 10, 515–527.
- (3) Tanaka, T.; Fillmore, D. J. *J. Chem. Phys.* **1979**, 70, 1214–1218.
- (4) Tierney, S.; Hjelme, D. R.; Stokke, B. T. *Anal. Chem.* **2008**, 80, 5086–5093.
- (5) Yin, J.; Dupin, D.; Li, J. F.; Armes, S. P.; Liu, S. Y. *Langmuir* **2008**, 24, 9334–9340.
- (6) Wang, J. P.; Gan, D. J.; Lyon, L. A.; El-Sayed, M. A. *J. Am. Chem. Soc.* **2001**, 123, 11284–11289.

- (7) Reese, C. E.; Mikhonin, A. V.; Kamenjicki, M.; Tikhonov, A.; Asher, S. A. *J. Am. Chem. Soc.* **2004**, *126*, 1493–1496.
- (8) Dupin, D.; Rosselgong, J.; Armes, S. P.; Routh, A. F. *Langmuir* **2007**, *23*, 4035–4041.
- (9) Zhang, Y. J.; Guan, Y.; Zhou, S. Q. *Biomacromolecules* **2006**, *7*, 3196–3201.
- (10) Hoare, T.; Pelton, R. *Macromolecules* **2007**, *40*, 670–678.
- (11) Luo, Q.; Guan, Y.; Zhang, Y.; Siddiq, M. J. *Polym. Sci., Polym. Chem.* **2010**, *48*, 4120–4127.
- (12) Yin, J.; Li, C. H.; Wang, D.; Liu, S. Y. *J. Phys. Chem. B* **2010**, *114*, 12213–12220.
- (13) Liu, P. X.; Luo, Q. F.; Guan, Y.; Zhang, Y. J. *Polymer* **2010**, *51*, 2668–2675.
- (14) Liu, Y.; Zhang, Y. J.; Guan, Y. *Chem. Commun.* **2009**, 1867–1869.
- (15) Kim, J. S.; Singh, N.; Lyon, L. A. *Angew. Chem., Int. Ed.* **2006**, *45*, 1446–1449.
- (16) Ogawa, K.; Wang, B.; Kokufuta, E. *Langmuir* **2001**, *17*, 4704–4707.
- (17) Wu, W.; Zhou, T.; Aiello, M.; Zhou, S. *Biosens. Bioelectron.* **2010**, *38*, 1343–1347.
- (18) Ding, Z. B.; Guan, Y.; Zhang, Y.; Zhu, X. X. *Soft Matter* **2009**, *5*, 2302–2309.
- (19) Shiino, D.; Murata, Y.; Kataoka, K.; Koyama, Y.; Yokoyama, M.; Okano, T.; Sakurai, Y. *Biomaterials* **1994**, *15*, 121–128.
- (20) Jung, D. Y.; Magda, J. J.; Han, I. S. *Macromolecules* **2000**, *33*, 3332–3336.
- (21) Kim, J. J.; Park, K. J. *Controlled Release* **2001**, *77*, 39–47.
- (22) Kataoka, K.; Miyazaki, H.; Bunya, M.; Okano, T.; Sakurai, Y. *J. Am. Chem. Soc.* **1998**, *120*, 12694–12695.
- (23) Ravaine, V.; Ancla, C.; Catargi, B. J. *Controlled Release* **2008**, *132*, 2–11.
- (24) Zhang, Y. J.; Guan, Y.; Zhou, S. Q. *Biomacromolecules* **2007**, *8*, 3842–3847.
- (25) Luo, Q.; Liu, P.; Guan, Y.; Zhang, Y. *ACS Appl. Mater. Inter.* **2010**, *2*, 760–767.
- (26) Lapeyre, V.; Gosse, I.; Chevreux, S.; Ravaine, V. *Biomacromolecules* **2006**, *7*, 3356–3363.
- (27) Hoare, T.; Pelton, R. *Biomacromolecules* **2008**, *9*, 733–740.
- (28) Lapeyre, V.; Ancla, C.; Catargi, B.; Ravaine, V. *J. Colloid Interface Sci.* **2008**, *327*, 316–323.
- (29) Wu, W. T.; Zhou, T.; Shen, J.; Zhou, S. Q. *Chem. Commun.* **2009**, 4390–4392.
- (30) Pelton, R. *Adv. Colloid Interface Sci.* **2000**, *85*, 1–33.
- (31) Christensen, M. L.; Keiding, K. *Colloid Surface A* **2005**, *252*, 61–69.
- (32) Weissman, J. M.; Sunkara, H. B.; Tse, A. S.; Asher, S. A. *Science* **1996**, *274*, 959–960.
- (33) Matsumoto, A.; Kurata, T.; Shiino, D.; Kataoka, K. *Macromolecules* **2004**, *37*, 1502–1510.
- (34) Ben-Moshe, M.; Alexeev, V. L.; Asher, S. A. *Anal. Chem.* **2006**, *78*, 5149–5157.
- (35) Asher, S. A.; Alexeev, V. L.; Goponenko, A. V.; Sharma, A. C.; Lednev, I. K.; Wilcox, C. S.; Finegold, D. N. *J. Am. Chem. Soc.* **2003**, *125*, 3322–3329.
- (36) Bradley, M.; Ramos, J.; Vincent, B. *Langmuir* **2005**, *21*, 1209–1215.
- (37) Shibayama, M.; Nagai, K. *Macromolecules* **1999**, *32*, 7461–7468.
- (38) Gan, T. T.; Guan, Y.; Zhang, Y. J. *J. Mater. Chem.* **2010**, *20*, 5937–5944.
- (39) Teverovsky, A. *Characteristic Times of Moisture Diffusion and Bake-out Conditions for Plastic Encapsulated Parts*, <http://nepp.nasa.gov/index.cfm/12753>.
- (40) Matsumoto, A.; Yoshida, R.; Kataoka, K. *Biomacromolecules* **2004**, *5*, 1038–1045.
- (41) Springsteen, G.; Wang, B. H. *Tetrahedron* **2002**, *58*, 5291–5300.
- (42) Lee, H. S.; Hong, J. J. *Biotechnol.* **2000**, *84*, 145–153.
- (43) Gaylord, N. G. *J. Polym. Sci. Polym. Symp.* **1968**, *24*, 1–5.
- (44) Morawetz, H. *Pure Appl. Chem.* **1974**, *38*, 267–277.
- (45) Sawant, S.; Morawetz, H. *Macromolecules* **1984**, *17*, 2427–2431.
- (46) Morawetz, H. *Acc. Chem. Res.* **1970**, *3*, 354–360.
- (47) Welsch, N.; Wittemann, A.; Ballauff, M. *J. Phys. Chem. B* **2009**, *113*, 16039–16045.
- (48) Frere, Y.; Gramain, P. *Macromolecules* **1992**, *25*, 3184–3189.
- (49) Hodge, P. *Chem. Soc. Rev.* **1997**, *26*, 417–424.
- (50) Lu, Y.; Mei, Y.; Drechsler, M.; Ballauff, M. *Angew. Chem., Int. Ed.* **2006**, *45*, 813–816.
- (51) Carregal-Romero, S.; Buurma, N. J.; Perez-Juste, J.; Liz-Marzan, L. M.; Hervas, P. *Chem. Mater.* **2010**, *22*, 3051–3059.
- (52) Huang, X.; Yin, Y. Z.; Tang, Y.; Bai, X. L.; Zhang, Z. M.; Xu, J. Y.; Liu, J. Q.; Shen, J. C. *Soft Matter* **2009**, *5*, 1905–1911.
- (53) James, T. D.; Sandanayake, K. R. A. S.; Iguchi, R.; Shinkai, S. *J. Am. Chem. Soc.* **1995**, *117*, 8982–8987.
- (54) Norrild, J. C.; Eggert, H. *J. Am. Chem. Soc.* **1995**, *117*, 1479–1484.